Fusicoccin A, a Phytotoxic Carbotricyclic Diterpene Glucoside of Fungal Origin, Reduces Proliferation and Invasion of Glioblastoma Cells by Targeting Multiple Tyrosine Kinases[1]

Marina Bury*, Anna Andolfi[†], Bernard Rogister[‡], Alessio Cimmino[†], Véronique Mégalizzi*, Véronique Mathieu*, Olivier Feron[§], Antonio Evidente[†] and Robert Kiss*

*Laboratoire de Toxicologie, Faculté de Pharmacie, Université Libre de Bruxelles, Brussels, Belgium; [†]Dipartimento di Scienze Chimiche, Complesso Universitario Monte Sant'Angelo, Napoli, Italy; [‡]Laboratoire de Neurobiologie du Développement, GIGA-Neurosciences, Université de Liège, Sart-Tilman B, Belgium; [§]Pole of Pharmacology and Therapeutics (UCL-FATH), Angiogenesis and Cancer Research Laboratory, Institut de Recherche Expérimentale et Clinique, Université Catholique de Louvain (UCL), Brussels, Belgium

Abstract

Glioblastoma multiforme (GBM) is a deadly cancer that possesses an intrinsic resistance to pro-apoptotic insults, such as conventional chemotherapy and radiotherapy, and diffusely invades the brain parenchyma, which renders it elusive to total surgical resection. We found that fusicoccin A, a fungal metabolite from *Fusicoccum amygdali*, decreased the proliferation and migration of human GBM cell lines *in vitro*, including several cell lines that exhibit varying degrees of resistance to pro-apoptotic stimuli. The data demonstrate that fusicoccin A inhibits GBM cell proliferation by decreasing growth rates and increasing the duration of cell division and also decreases two-dimensional (measured by quantitative video microscopy) and three-dimensional (measured by Boyden chamber assays) migration. These effects of fusicoccin A treatment translated into structural changes in actin cytoskeletal organization and a loss of GBM cell adhesion. Therefore, fusicoccin A exerts cytostatic effects but low cytotoxic effects (as demonstrated by flow cytometry). These cytostatic effects can partly be explained by the fact that fusicoccin inhibits the activities of a dozen kinases, including focal adhesion kinase (FAK), that have been implicated in cell proliferation and migration. Overexpression of FAK, a nonreceptor protein tyrosine kinase, directly correlates with the invasive phenotype of aggressive human gliomas because FAK promotes cell proliferation and migration. Fusicoccin A led to the down-regulation of FAK tyrosine phosphorylation, which occurred in both normoxic and hypoxic GBM cell culture conditions. In conclusion, the current study identifies a novel compound that could be used as a chemical template for generating cytostatic compounds designed to combat GBM.

Translational Oncology (2013) 6, 112–123

Introduction

Glioblastoma multiforme (GBM; World Health Organization grade IV) is the most common malignant primary brain tumor in adults and children and is associated with a dismal prognosis. The mean survival time after the current standard treatment that includes a combination of neurosurgery, radiotherapy, and concomitant chemotherapy with temozolomide (TMZ) is only 15 months [1–3]. The low survival rate for patients with GBM reflects the inability to achieve total surgical

resection, mainly because GBM cells possess the ability to invade the surrounding normal brain and have a high propensity for recurrence [2–5]. GBMs are characterized by a number of genetic and signaling abnormalities that ultimately lead to uncontrolled cellular proliferation and invasion, angiogenesis, necrosis, and resistance to cytotoxic therapies [2–5]. Among these aberrancies are an abnormal activation of the phosphatidylinositol 3-kinase (PI3K)/AKT and Ras/Raf/mitogen-activated protein kinase (MAPK) signal transduction pathways [2]. Therefore, to improve the prognosis of patients with GBM, it is essential to find novel therapeutic agents that can manage the growth, invasion, and progression of these tumor cells by interfering with signaling molecules or pathways that are critical for the malignant phenotype of gliomas, including GBMs. Numerous clinical trials are currently investigating the benefits of synthetic agents called targeted therapeutics [6–8].

Natural products are a valuable resource that could yield novel efficacious anticancer agents [9,10]. Various attempts have been made to treat GBM patients with paclitaxel [11], a microtubule inhibitor, or with irinotecan [12], a topoisomerase inhibitor, but these drugs have had limited success, even when locally delivered to bypass the blood-brain barrier. These compounds are cytotoxic and rapidly induce GBM chemoresistance processes, including the activation of the multidrug resistance phenotype [13]. In our research programs, we are searching for novel natural compounds that display 1) growth inhibitory effects in malignant glioma cells that exhibit varying degrees of resistance to pro-apoptotic stimuli, 2) cytostatic rather than cytotoxic effects, and 3) bioselectivity between normal and tumor glial cells. The current study shows that fusicoccin A fits these various criteria.

Fusicoccin A is the α-D-glucopyranoside of a carbotricyclic diterpene (Figure 1) that is the main phytotoxin produced by *Fusicoccum amygdali*, the causative fungal agent of peach and almond canker [14]. Several reports have previously described the biologic effects of fusicoccin A in plant and mammalian cells. Fusicoccin A activates
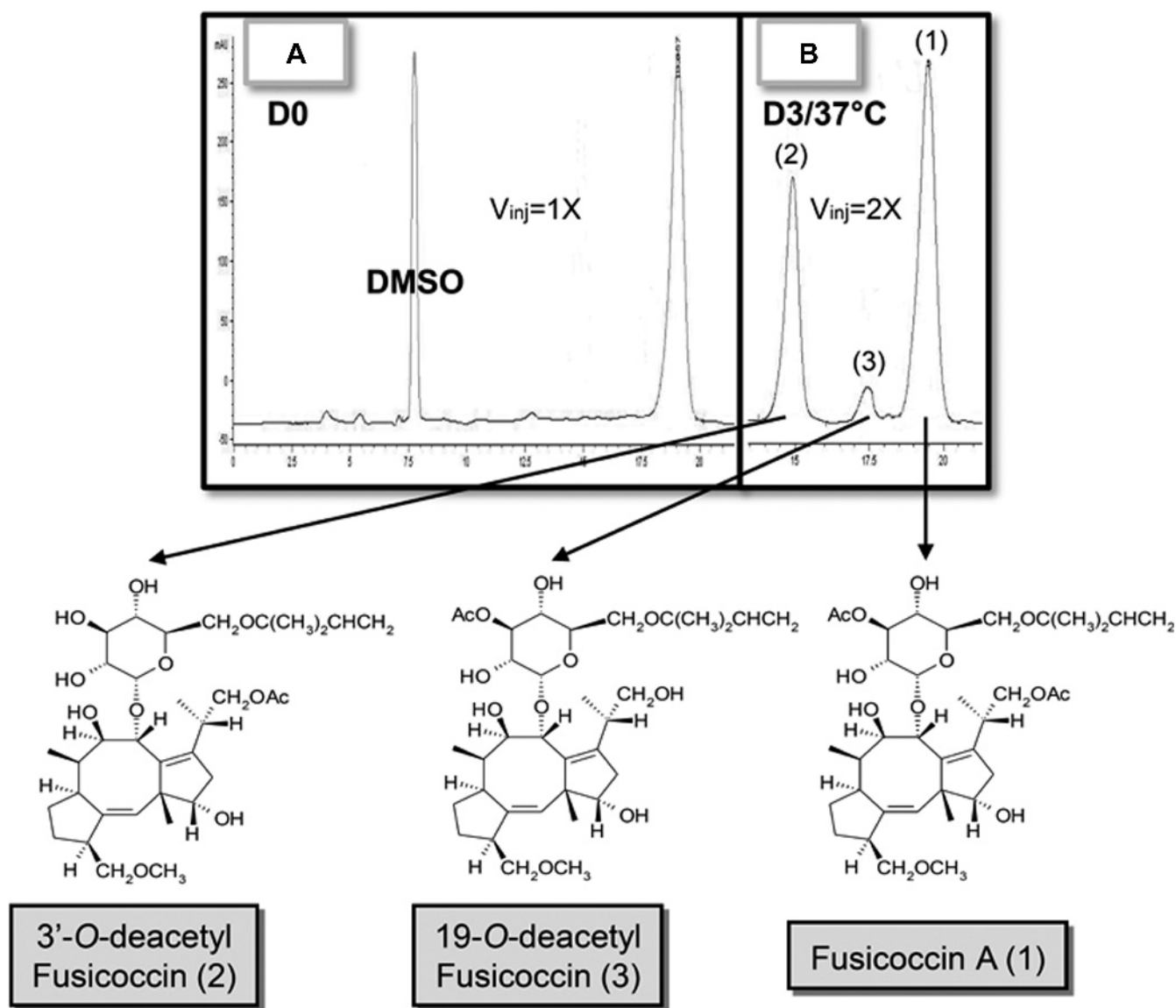

Figure 1. Physicochemical stability of fusicoccin A. The determination of fusicoccin A (1) physicochemical stability and the identification of its two major degradation products [3'-O-deacetyl fusicoccin (2) and 19-O-deacetyl fusicoccin (3)] when maintained for 3 days (B) at 37°C in MEM compared to day 0 (A).

the plasma membrane H^+-ATPase by stabilizing its binding to 14-3-3 proteins, which results in water loss and the wilting of infected plants [15]. Bunney et al. [16] demonstrated that fusicoccin A–related signaling reveals 14-3-3 protein function as a novel step in left-right patterning during amphibian embryogenesis. Fusicoccin A also targets 14-3-3 proteins in cancer cells [17] and it promotes isoform-specific expression of 14-3-3 proteins in human gliomas [18]. Takahashi et al. [17] found that these 14-3-3 proteins play a critical role in serine/threonine kinase–dependent signaling pathways through protein-protein interactions with multiple phosphorylated ligands. Fusicoccin A also induces apoptosis in tumor cells by activating the tumor necrosis factor–related apoptosis-inducing ligand pathway when it is applied to cells after or combined with interferon-α priming [19]. Here, we report the bioselective effects of fusicoccin A between normal and tumor glial cells, with fusicoccin A–mediated targeting of several kinases (that are implicated in the actin cytoskeleton organization) and a special emphasis on focal adhesion kinase (FAK), which is implicated in GBM cell proliferation and migration phenotypes.

Materials and Methods

Fusicoccin A, 3′-O-Deacetyl Fusicoccin A, and 19-O-Deacetyl Fusicoccin A

Fusicoccin A was harvested from *F. amygdali* as reported previously [20,21]. Fusicoccin A samples were purified by column chromatography [eluent $CHCl_3$-*iso*-PrOH (9:1)] and crystallized from EtOAc–*n*-hexane as detailed previously [21]. The electrospray ionization–mass spectrometry (ESI-MS) spectrum of the major degradation product revealed a molecular sodium cluster at 661 *m/z*, which corresponded to 3′-O-deacetyl fusicoccin A and this result was confirmed by the ^1H nuclear magnetic resonance (NMR) and electron impact–mass spectrometry (EI-MS) spectra. The minor degradation product's ESI-MS spectrum displayed sodium and potassium cluster ions at *m/z* 661 and 677, respectively. These data completed by ^1H NMR analyses enabled the identification of the structure as 19-O-deacetyl fusicoccin A.

To obtain sufficient amounts of these two degradation products to test their *in vitro* growth inhibitory concentrations in glioma cell lines (see below), both products were obtained from the deacetylation of fusicoccin A. Fusicoccin A (100 mg) was dissolved in 250 ml of MeOH and left at 37°C for 1 week. Next, the solvent was evaporated under reduced pressure and the residue was purified by preparative thin-layer chromatography (TLC) and eluted with solvent system A (see below) to yield 3′-O- and 19-O-deacetylfusicoccin A as amorphous solids (70 and 9 mg, respectively).

Physicochemical Stability Analyses

Fusicoccin A stability in minimal essential cell culture medium (MEM) was characterized at 37°C for 3 days. Fusicoccin A (100 μg/ml) was prepared by diluting a DMSO stock solution in MEM (Invitrogen, Merelbeke, Belgium). After 3 days of incubation at 37°C, the solution was diluted with the appropriate solvent (see below) at 1 μg/ml final concentration for analysis. For improved observation of the degradation peaks, the volume injected into high-performance liquid chromatography (HPLC) D3 (V_{inj} = 2X) was doubled compared to D0 (V_{inj} = 1X). The chromatograms were recorded on Agilent Technologies 1200 series with a UV-VIS detector. The column used for this analysis was a C-18 HD, the solvent was CH_3OH/H_2O (7:3), the flow rate was 0.5 ml/min, and λ = 220 nm. Analytical and preparative TLCs were performed on silica gel (Merck, Darmstadt, Germany; Kieselgel 60 F_{254}, 0.25 and

0.50 mm, respectively). The spots were visualized by exposure to UV light and/or by first spraying them with a 10% H_2SO_4 solution in MeOH and then with 5% phosphomolybdic acid in ethanol, which was followed by heating at 110°C for 10 minutes. Solvent system (A) was $CHCl_3$-*i*-PrOH (93:7). ^1H NMR spectra were recorded at 400 MHz in $CDCl_3$ by Bruker spectrometers. ESI-MS spectra were recorded on Agilent Technologies 1100 series quadrupole 6120 and the EI-MS spectra were taken at 70 eV on a QP 5050 Shimadzu spectrometer.

Cell Lines, Culture Conditions, and Transfection

Cancer cell lines were obtained from the American Type Culture Collection (ATCC, Manassas, VA). The U373-MG (ATCC code HTB-17) human glioblastoma, the Hs683 (ATCC code HTB-138) human oligodendroglioma, and the B16F10 (ATCC code CRL-6475) mouse melanoma cell lines were cultured in RPMI (Invitrogen) culture media supplemented with 10% heat-inactivated fetal calf serum (FCS; Invitrogen), 4 mM glutamine, 100 μg/ml gentamicin, and penicillin-streptomycin (200 U/ml and 200 μg/ml; Invitrogen) at 5% CO_2, 21% O_2, and 37°C. Hypoxia (1% O_2) was achieved as previously described [22]. For FAK overexpression, pCMV6-PTK2 (FAK) and pCMV6-XL4 (control) from OriGene (Rockville, MD) were transfected into U373-MG cells with TurboFect (Fermentas, Waltham, MA) as previously described [23]. Transfected cells were selected with G418 (Invitrogen) at 300 μg/ml during 2 weeks. All cancer cell lines used in this work have been previously cultured with DMSO concentrations up to 5% without any modifications in their growth levels when compared to control cells.

Normal astrocytes were obtained from neonatal nuclear magnetic resonance imaging (NMRI) mouse cortices that were freed of meninges, minced into small pieces of tissue with microscissors, and then suspended in MEM (Invitrogen) supplemented with 6 g/l glucose and 10% FCS (Invitrogen). The cell suspension was then filtered through 225- and 25-μm pore filters. The filtered cell suspension was plated on an uncoated T25 flask for 72 hours. The medium was then changed and the cells were grown until confluence. Control astrocytes were exposed to the percentages of DMSO used in fusicoccin A–related treated conditions.

Cell Growth Inhibition Assay

The colorimetric 3-(4,5-dimethylthiazol-2-yl)-2,5-diphenyltetrazolium bromide (MTT) viability assay (Sigma, Bornem, Belgium) was used to determine the overall growth rate of each cell line as previously described [24]. The number of living cells was determined after 72 hours of culture in the presence of fusicoccin A, 3′-O-deacetyl fusicoccin A, or 19-O-deacetyl fusicoccin A. Fusicoccin A was also tested on mouse astrocytes. Each experimental condition was performed in triplicate.

To investigate whether fusicoccin A–induced growth inhibitory effects in glioma cells were irreversible or not, U373-MG and Hs683 cells were treated with 100 μM fusicoccin A and were washed after 3, 24, and 48 hours after treatment. The number of viable cells was determined 72 hours after having removed fusicoccin A from the culture media. Each experimental condition was performed in six replicates.

Computer-assisted Phase-Contrast Microscopy (Video Microscopy)

Using the human U373-MG GBM cell line, the effects of treatment with 100 μM fusicoccin A on cell viability and cell division were characterized *in vitro* by computer-assisted phase-contrast video microscopy as described elsewhere [25]. The cells were monitored for 72 hours.

Films were compiled from the obtained time-lapse image sequences, which enabled a rapid screening of cell viability. Each experimental condition was performed in triplicate.

Cell count–based determination of global growth ratio.   In each (control or treated) condition, the cell growth rate was evaluated by the ratio between the number of cells counted in the first and last frames of the image sequences. The global growth ratio (GGR) was defined as the ratio between the two growth levels obtained in the treated and control conditions. All of the cell counts were performed in triplicate using an interactive computer tool [25,26]. The GGRs were computed at the 24th, the 48th, and the 72nd hour of quantitative video microscopy analyses by dividing the cell growth rate in fusicoccin A–treated U373-MG cell populations by the cell growth rate at the same experimental times in the corresponding control U373-MG cell populations.

Specific analysis of cell division rate and duration.   Cells undergoing division exhibit very bright patterns compared to nondividing cells. On the basis of this observation, we developed a custom division detection system that is capable of identifying cells undergoing division in time-lapse sequences. This detection method is based on an automatic event detection completed by an interactive validation/correction procedure as previously described [25,26]. At the end of the sequence analysis, all of the events are linked to different cell divisions, which reveal the number of cell divisions as well as their durations [25,26]. We computed the cell division numbers normalized by the number of cells that were counted in the first frame.

Quantitative determination of cell migration.   The effect of fusicoccin A (100 μM) on cell motility in the U373-MG GBM cell line was investigated. Figure 5A shows typical analyses based on the individual cell trajectories that are established by a cell-tracking algorithm based on an image series acquired during a cell migration experiment. The greatest linear distance between a starting point of a cell and the farthest point reached in its trajectory, also known as the maximum relative distance from the point of origin (MRDO), was the quantitative variable used to characterize compound-mediated effects on cancer cell migration [27].

Determination of In Vitro Cell Death

To evaluate viability in U373-MG cells that were treated with fusicoccin A, an assay measuring DNA fragmentation was used. The terminal deoxynucleotidyl transferase–mediated deoxyuridine triphosphate nick end labeling (TUNEL) assay was performed according to a procedure previously described [28,29] using the APO-Direct Kit (BD Pharmingen, Erembodegem-Aalst, Belgium). The protocol was performed according to the manufacturer's instructions, including the use of positive and negative controls. Briefly, U373-MG GBM cells were treated with 100 μM fusicoccin A for either 24 or 72 hours in culture media or left untreated. Adherent and nonadherent cells were collected, fixed with 1% paraformaldehyde (1 hour) at 4°C, permeabilized, and stored in 70% ethanol at –20°C. TUNEL labeling was performed for 1 hour at 37°C and the stained cells were analyzed on a CellLab Quanta SC flow cytometer (Beckman Coulter, Analis, Suarlee, Belgium).

Analyses of Actin Cytoskeletal Organization

U373-MG cells were cultured for 30 hours in the absence (controls) or presence of 100 μM fusicoccin A on glass coverslips as previously described [30]. Fluorescent phalloidin conjugated with the Alexa Fluor 488 fluorochrome (Molecular Probes, Invitrogen) was used to label fibrillar actin, and Alexa Fluor 594–conjugated DNAse I (Molecular Probes, Invitrogen) was used to stain globular actin. The coverslips were mounted on microscope slides with 10 μl of Moviol agent (Calbiochem, VWR, Heverlee, Belgium). Three coverslips per experimental condition were analyzed and three pictures were taken for each coverslip (with the same exposure time) using an AxioCamHRm fluorescent microscope (Zeiss, Oberkochen, Germany). The most representative images are shown in Figure 4B.

Boyden Chamber Assay

The invasive features of U373-MG cells treated with 50 and 100 μM fusicoccin A for 24 hours *in vitro* were assessed using the Boyden transwell invasion system (BD BioCoatMatrigel invasion chambers; BD Biosciences Discovery Labware, Bedford, MA) as detailed elsewhere [31]. In parallel, the same number of U373-MG cells were seeded in 24-well plates coated with Matrigel, and we treated the cells with 0 (control), 50, or 100 μM fusicoccin A for 24 hours. To normalize the number of invasive cells, the number of viable cells in each condition was determined. Each experiment was performed in triplicate.

In Vitro Adhesion Assay

The adhesion assay was performed as described previously [31] with modifications. Briefly, glass coverslips in 24-well plates were precoated with Matrigel (diluted 1:3 in RPMI culture media with 10% FCS) for 1 hour at 37°C. The wells were washed and nonspecific binding was then blocked with 0.1% BSA in phosphate-buffered saline for 30 minutes. U373-MG cells (20,000 cells per well) were allowed to adhere for 24 hours at 37°C in the presence of either 0 (control), 50, or 100 μM fusicoccin A, after which nonadherent cells were gently washed away with warm phosphate-buffered saline. Adherent cells were methanol-fixed, hematoxylin-stained, and counted in 10 fields per well at a G × 10 magnification using an Olympus microscope (Olympus, Antwerp, Belgium). Each experimental condition was performed in triplicate.

Kinase Activity Determination

We originally provided ProQinase (Freiburg, Germany) with fusicoccin A as a stock solution in 100% DMSO and aliquots were further diluted with water in 96-well microliter plates directly before use. A radiometric protein kinase assay (^{33}PanQinase Activity Assay) was used for measuring the kinase activity of 288 recombinant protein kinases as detailed previously [32]. Fusicoccin A was tested in two replicates in each kinase assay, and the final concentration tested was 50 μM.

Western Blot Analyses

U373-MG cells, either untreated (control) or treated with 25, 50, or 100 μM fusicoccin A, were incubated under normoxic or hypoxic conditions (see the Cell Lines, Culture Conditions, and Transfection section). U373-MG cells were also treated with 100 μM $CoCl_2$ for 4 hours as a positive control for the expression of hypoxia-inducible factor-1alpha (HIF-1α). Proteins were extracted using the CelLytic M Cell Lysis Reagent (Sigma) with 1 mM Na_3VO_4. An equal amount of cell extract was resolved on a sodium dodecyl sulfate–polyacrylamide gel electrophoresis (SDS-PAGE) gel and transferred to a polyvinylidene fluoride (PVDF) membrane. The membranes were blocked with 5% milk or BSA for at least 1 hour, followed by an overnight incubation

at 4°C with the following primary antibodies: phosphorylated FAK (diluted 1:100; R&D Systems, Minneapolis, MN), FAK (diluted 1:100; R&D Systems), HIF-1α (diluted 1:200; Abcam, Cambridge, United Kingdom), and tubulin (diluted 1:5000, Abcam). Secondary antibodies were purchased from Pierce (Aalst, Belgium) and the blots were analyzed using the Bio-Rad ChemiDoc XRS Imager and were quantified with Image Lab (Bio-Rad Laboratories, Nazareth Eke, Belgium). The experiments were performed in two independent replicates.

Statistical Analysis

The data obtained from two independent groups were compared using the nonparametric Mann-Whitney U test. The statistical analysis was performed using Statistica software (StatSoft, Tulsa, OK). When the number of experiments was less than $n = 4$, the mean ± SD was used.

Results

Characterization of Fusicoccin A Physicochemical Stability

Figure 1 shows that fusicoccin A [retention time (RT) = 19.5 minutes] generates two degradation products when it is maintained at 37°C for 3 days in MEM culture media. The major degradation product has been identified (with comparisons to the available standards) as 3′-O-deacetyl fusicoccin (RT = 14.7 minutes) and the minor product as 19-O-deacetyl fusicoccin (RT = 17.4 minutes) using TLC, HPLC,

ESI-MS, EI-MS, and NMR analyses according to a methodology that was previously validated [21]. The ESI-MS spectra of these degradation products revealed a molecular sodium cluster at 661 m/z, which corresponded to 3′-O-deacetyl fusicoccin A, and sodium/potassium cluster ions at m/z 661 and 677, which corresponded to 19-O-deacetyl fusicoccin A, confirmed by the EI- and ESI-MS and ^{1}H NMR. HPLC analyses revealed that approximately 50% of fusicoccin A remained after 3 days (D3) at 37°C in MEM (Figure 1B). The *in vitro* growth inhibitory activities of fusicoccin A, 3′-O-deacetyl fusicoccin A, and 19-O-deacetyl fusicoccin A were determined by calculating the means from the MTT colorimetric assay performed on U373-MG and Hs683 glioma cell lines as detailed below.

In Vitro Growth Inhibitory Effect of Fusicoccin A in Normal versus Cancer Cell Lines

The *in vitro* growth inhibitory activity of fusicoccin A and its two degradation products was assayed using an MTT colorimetric assay on two human glioma cancer cell lines (Figure 2A). The U373-MG cancer cell line displays varying degrees of resistance to pro-apoptotic stimuli [33], while the human Hs683 oligodendroglioma cell line (1p19q co-deleted) displays sensitivity to pro-apoptotic stimuli [34]. The inhibitory effect of fusicoccin A on *in vitro* growth was also analyzed in normal astrocytes (Figure 2B). We observed no differences in terms of sensitivity to fusicoccin A and its degradation products between the two glioma cell lines with distinct sensitivities to pro-apoptotic stimuli. We identified the *in vitro* concentration of each
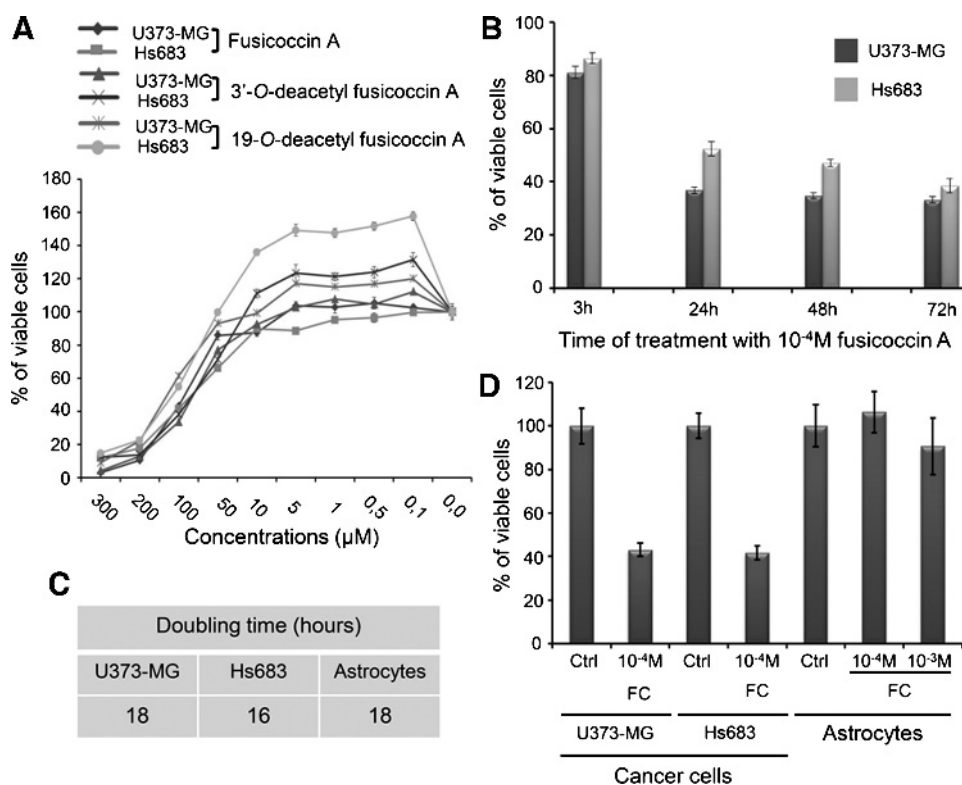

Figure 2. Anticancer activity of fusicoccin A and its degradation products. (A) Characterization of the *in vitro* growth inhibitory effects induced by fusicoccin A, 3′-O-deacetyl fusicoccin, and 19-O-deacetyl fusicoccin in two human glioma cell lines (U373-MG and Hs683). (B) Characterization of the *in vitro* growth inhibitory effects induced by 100 μM fusicoccin A 72 hours after having cultured the cancer cells for 3, 24, and 48 hours before washing out fusicoccin A. (C) Doubling time of U373-MG and Hs683 glioma cells *versus* normal astrocytes. (D) Determination of fusicoccin A–related bioselectivity between normal (astrocytes) and tumor (Hs683 and U373-MG) cells using the MTT colorimetric assay.
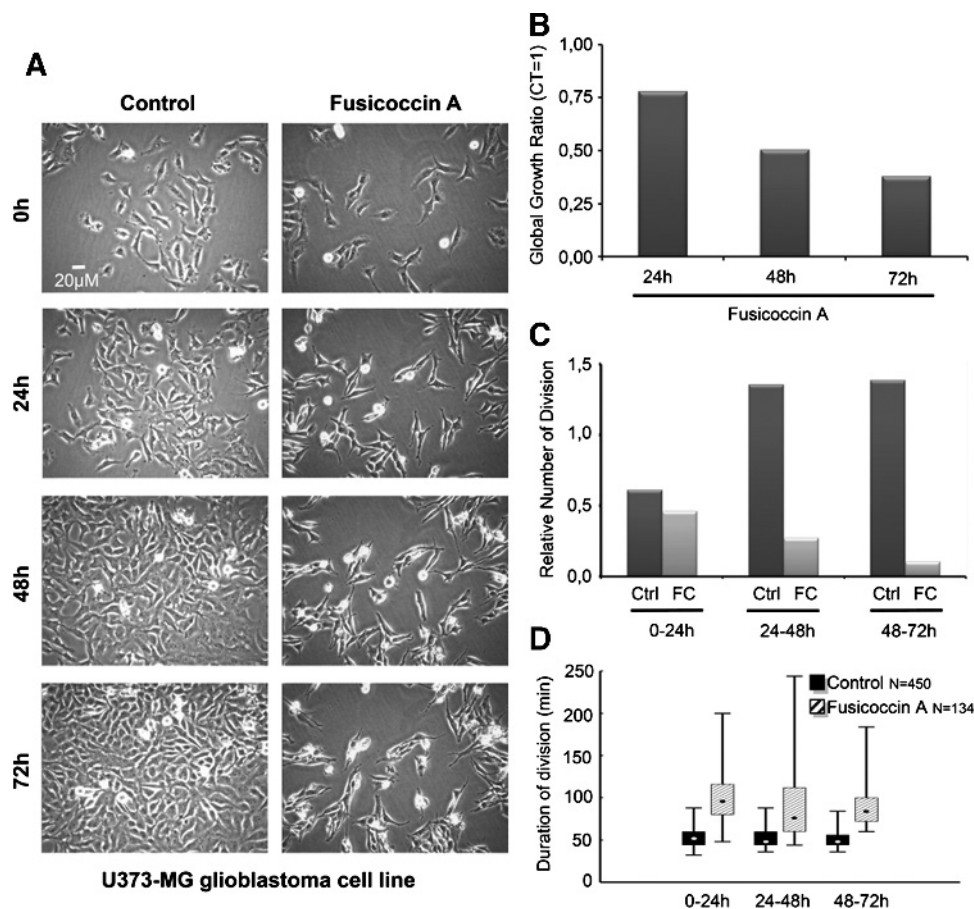
Figure 3. Fusicoccin A decreases proliferation of GBM cells. (A) Video microscopy–related illustrations of the effects of 100 μM fusicoccin A on the U373-MG GBM cell line after 72 hours. (B) *In vitro* global growth rate determination (using the GGR assessment as described in Materials and Methods section) of fusicoccin A–treated U373-MG cells compared to their control counterparts. (C) The number of cell division events detected during the 0- to 24-, 24- to 48-, and 48- to 72-hour treatments of U373-MG cells with 100 μM fusicoccin A. The relative number of divisions is the number of cell divisions counted and normalized by the number of cells counted in the first frame. (D) The duration of cell division events detected during the 0- to 24-, 24- to 48-, and 48- to 72-hour treatments of U373-MG cells with 100 μM fusicoccin A. The data are reported as the median values $\pm$ the 25th to 75th percentiles calculated in triplicate.

of the three compounds that induced a 50% reduction in growth (IC$_{50}$) after culturing the cells for 3 days either in the presence or the absence (control) of the drug of interest: the IC$_{50}$ growth inhibitory concentration of fusicoccin A was 92 μM in the U373-MG cells and 83 μM in the Hs683 glioma cells, whereas the IC$_{50}$ ranged between 80 and 130 μM for the two degradation products in these two glioma cell lines (Figure 2A). Therefore, we focused on fusicoccin A and its potential anti-GBM effects, which become irreversible after 24 hours of treatment (Figure 2B). For assessment of differential sensitivity between normal and tumor glial cells to fusicoccin A, normal astrocytes showing similar doubling time as cancer cells under study were used (Figure 2C). We observed that 1 mM fusicoccin A treatment did not significantly decrease the growth of normal astrocytes, whereas 100 μM fusicoccin A treatment decreased the growth of the two tumor glial cell lines by approximately 50% (Figure 2D). As the inhibitory activity of fusicoccin A on *in vitro* growth was analyzed in human glioma cell lines while the bioselectivity was determined in normal mouse astrocytes, we also determined that fusicoccin A inhibited *in vitro* growth with an IC$_{50}$ of ~70 μM in mouse melanoma B16F10 cells to rule out differences that could relate to interspecies features. This result indicates that mouse and human cancer cells dis-

play similar sensitivity to fusicoccin A. Therefore, the bioselectivity index between normal and tumor astrocytes is >10.

Fusicoccin A Displays Cytostatic Effects through an Increase in the Duration of Cell Division in GBM Cells

Fusicoccin A induces cytostatic effects in U373-MG GBM cells, which is demonstrated in Figure 3A. Using quantitative video microscopy analyses, we validated the growth inhibitory effects of fusicoccin A on U373-MG cells that were observed in the MTT colorimetric assay. Indeed, Figure 3B shows that fusicoccin A–treated U373-MG cells displayed lower growth kinetic rates over time when compared with control cells as measured by calculating GGR indices. According to these GGR index calculations, 100 μM fusicoccin A treatment for 72 hours decreased the *in vitro* growth rate of U373-MG GBM cells by approximately 60% (GGR = 0.4). Quantitative video microscopy analyses also revealed that the growth inhibitory activity of fusicoccin A was essentially due to cytostatic effects, including a marked decrease in the mitotic rate of U373-MG GBM cells (Figure 3B) and an increased duration of cell division (Figure 3C). Indeed, the cell division duration increased by 40 minutes in U373-MG GBM cells over the

72-hour period of 100 µM fusicoccin A treatment compared to control cells ($P < .001$).

Fusicoccin A–treated U373-MG GBM Cells Display Marked Modifications in the Actin Cytoskeletal Organization and Few Cell Deaths Only

The morphologic changes observed in Figure 4A (a arrows) show an elongated morphology of the U373-MG cells, suggesting cytoskeletal changes. Fluorescence microscopy analyses confirmed that fusicoccin A induced modifications in the actin cytoskeletal organization in these cells (Figure 4B). Indeed, the levels of polymerized actin (green fluorescence) increased in U373-MG GBM cells after 30 hours of 100 µM fusicoccin A treatment (Figure 4B). In contrast, as morphologically illustrated in Figure 4A (b arrows), few cell deaths occur over the 72-hour period of fusicoccin A treatment as confirmed by flow cytometry (FCM)/TUNEL analyses. The data in Figure 4C show that fewer than 20% of the U373-MG cells treated with 100 µM fusicoccin A for 72 hours underwent DNA degradation processes.

Fusicoccin A Affects the Migration Characteristics of U373-MG GBM Cells

The dynamic organization of the F-actin cytoskeleton and the regulation of focal adhesion assembly and disassembly are essential processes required for efficient movement in cell migration. There-fore, we analyzed the effects of fusicoccin A on the migration of U373-MG cells. As shown in Figure 5, A and B (quantitative video microscopy), fusicoccin A decreased both two-dimensional and three-dimensional (Figure 5, C and D; Boyden chamber assay) migration features of U373-MG GBM cells. The reduction in the number of invading cells was not due to a decrease in cell proliferation or cytotoxicity because 1) as shown in Figure 5D, the number of invading cells was normalized by the number of living cells counted in both the control and fusicoccin A–treated conditions after a 24-hour period and 2) we show that fusicoccin A also decreased the adhesion of U373-MG cells cultured on Matrigel in a dose-dependent manner (Figure 5, E and F).

Fusicoccin A Inhibits the Activity of Various Kinases, Including FAK

Actin cytoskeletal organization and the invasive and adhesive characteristics of cells, in particular GBM cells, depend on multiple signaling pathways, including various protein kinases [35,36]. At 50 µM, a concentration we tested in the invasion and adhesion assays (Figure 5) that is weaker than the *in vitro* IC_{50} growth inhibitory concentrations (92 µM in U373-MG and 83 µM in Hs683 glioma cells), fusicoccin A decreased the activities of 13 (Figure 6A) of 288 kinases analyzed by 50%, especially tyrosine kinase (Figure 6B). As detailed later in the Discussion section, of these 13 kinases targeted by fusicoccin A, we
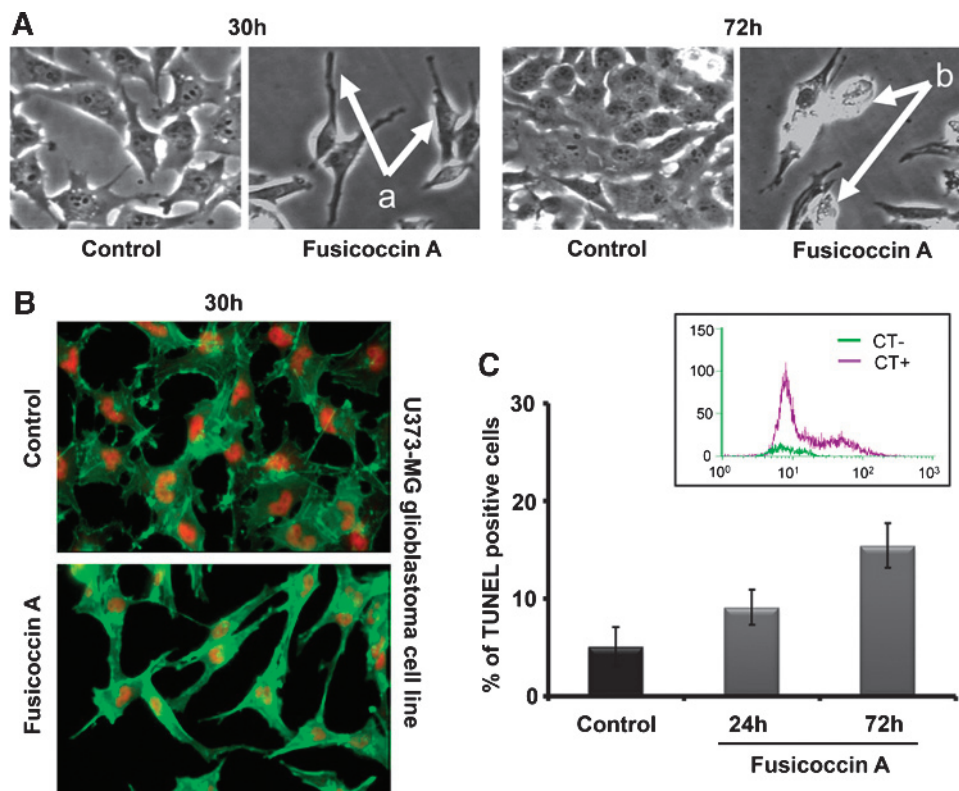

Figure 4. Fusicoccin A is a cytostatic compound. (A) The panel represents illustrations of the morphologic changes of U373-MG cells treated with 100 µM fusicoccin A after 30 and 72 hours compared to the untreated cells; a arrows represent the elongation of U373-MG cells treated with fusicoccin A after 30 hours and b arrows indicate dead cells after 72 hours. (B) Fluorescence microscopy was employed to visualize the fibrillar (polymerized) actin in green and the globular (unpolymerized) actin in red. The effects of 100 µM fusicoccin A were monitored during 30 hours and compared to untreated cells. (C) FCM-related analyses (TUNEL) of the percentages of apoptotic U373-MG GBM cells that were treated for 24 and 72 hours with 100 µM fusicoccin A. The positive and negative controls were furnished by the manufacturer of the TUNEL kit and are presented above the graph. The data are reported as the mean values ± SD calculated in triplicate.
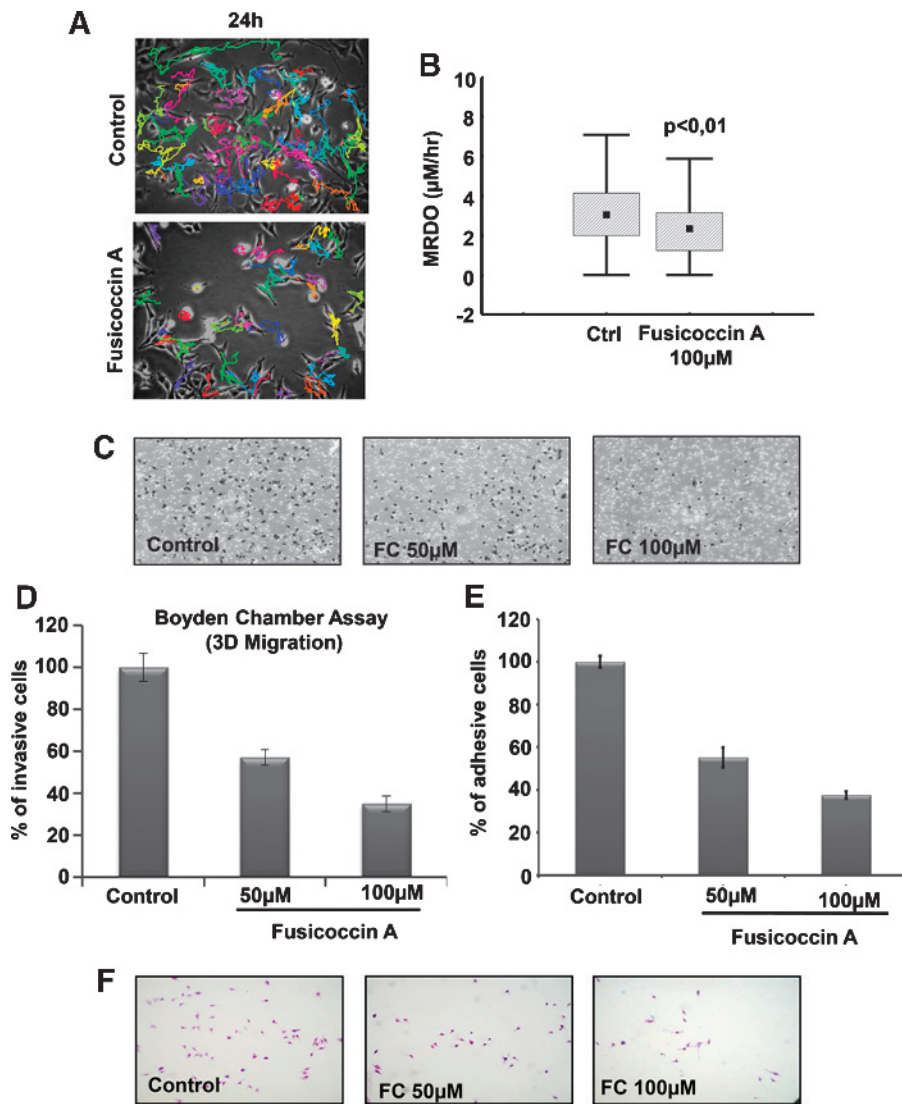
Figure 5. Fusicoccin A decreases migration of GBM cells. (A) The evaluation of the antimotility activity of fusicoccin A in U373-MG GBM cells. The motility of individual cells treated with 100 μM fusicoccin A for 24 hours was quantified by establishing the trajectory of each cell centroid and by quantifying the MRDO variable (the maximum distance covered by a cell and normalized by its observation time, expressed in μm/h). (B) The distribution of MRDO values obtained for U373-MG cells treated with 100 μM fusicoccin A for 24 hours compared to the untreated cells. The data are reported as the median values $\pm$ the 25th to 75th percentiles calculated in triplicate. (C) The panel represents illustrations of the U373-MG invasive cells that were either untreated or treated with 50 or 100 μM fusicoccin A for 24 hours. (D) Quantification of the *in vitro* invasive activity of U373-MG cells either untreated or treated with fusicoccin A in Boyden chambers coated with Matrigel. The cells that penetrated through the Matrigel to the lower surface of the filters were stained. The number of invasive cells was counted in 10 fields per chamber (the chamber surface includes 30 fields), and the experiment was conducted in triplicate. The sum of the 10 values was used to calculate the percentage of invasive cells in the population, and the control invasion rate was normalized to the number of counted cells as 100%. We also normalized the invasion rate by the number of counted cells treated with 50 and 100 μM fusicoccin A. The results are expressed as the mean values $\pm$ SD calculated in triplicate. (E) Quantification of the *in vitro* adhesive activity of U373-MG cells that were either untreated or treated with fusicoccin A. The cells that adhered on Matrigel supports were stained and then determined by microscopy. The number of adhesive cells was counted in 10 fields per glass coverslip and the experiment was conducted in triplicate. The sum of the 10 values was used to calculate the percentage of adhesive cells in the population, and the control adhesion rate was reported to be 100%. The results are expressed as the mean values $\pm$ SD calculated in triplicate. (F) The panel represents illustrations of the U373-MG adhesive cells either untreated or treated with 50 or 100 μM fusicoccin A for 24 hours.

focused specifically on FAK because 1) it is an important player in the acquisition of the aggressive phenotype of GBM cells and 2) our data show FAK's potential implication in the defect of cell adhesion (Figure 5E). Moreover, FAK is implicated in proliferation, morphology modification, migration, invasion, adhesion, angiogenesis, and cancer cell survival features [37–44].

Fusicoccin A Inhibits FAK Phosphorylation of U373-MG GBM Cells in Both Normoxic and Hypoxic Conditions

FAK is activated by autophosphorylation of tyrosine 397, which is necessary for FAK-induced cell invasion [37–40]. To determine whether FAK is involved in the fusicoccin A–induced inhibition of U373-MG cell invasion and adhesion, we performed immunoblot

experiments using a phosphorylation-specific antibody against FAK in both normoxic and hypoxic cell culture conditions. We analyzed FAK activity in both normoxic and hypoxic conditions because it has been previously shown that the activated form of FAK is increased in GBM cells grown in hypoxic conditions [43] [see also phosphorylated focal adhesion kinase (pFAK) signals in normoxic *versus* hypoxic conditions in untreated cells in Figure 7*C*].

First, we determined whether the *in vitro* IC$_{50}$ of fusicoccin A in U373-MG cells (as determined above) differed in normoxic *versus* hypoxic conditions. As shown in Figure 7*A*, this was not the case. In addition, as shown in Figure 7*C*, at concentrations ranging from 25 to 100 μM, fusicoccin A reduced FAK phosphorylation at tyrosine 397 under both normoxic and hypoxic conditions in a dose-dependent manner. We also verified that hypoxic conditions were actually induced

in U373-MG GBM cells by confirming the increase in HIF-1α expression in GBM cells maintained under 1% O$_2$ conditions (Figure 7*B*).

FAK Overexpression in U373-MG Cells Reduces Fusicoccin A–Induced Growth Inhibition

To confirm that FAK is actually associated with the *in vitro* growth inhibitory activity of fusicoccin A, U373-MG cells were transfected with pCMV6-PTK2 (FAK) or with pCMV6-XL4 (control) and then their growth levels in the presence or the absence (control) of fusicoccin A was evaluated by means of the MTT colorimetric assay. FAK overexpression after transfection was confirmed by Western blot analysis (Figure 7*D*). As shown in Figure 7*E*, FAK overexpression in U373-MG cells reduced by about two times the *in vitro* growth inhibitory effects induced by fusicoccin A.

Discussion

GBM is currently an incurable disease with a median survival time of approximately 15 months [3]. The search for low–molecular weight drugs that target growth-related kinases, especially tyrosine kinases, has become an attractive area of research that aims to identify new therapies that can extend the survival and standard of life of patients with cancer [36]. In this report, fusicoccin A was identified as an inhibitor of several kinases, including FAK. Because FAK is a key molecule that is necessary for cell proliferation, migration, angiogenesis, and invasion during cancer progression [37–44], FAK, in addition to other kinases implicated in the control of the actin cytoskeletal organization, could potentially be a target in GBMs [45].

In the current study, the anticancer activity of fusicoccin A, a phytotoxic carbotricyclic diterpene glucoside of fungal origin, was characterized in glioma cells. First, we analyzed whether fusicoccin A displays bioselectivity between normal and tumor glial cells, and the data clearly indicated that the bioselectivity level is at least above 10. The bioselectivity of fusicoccin A therefore suggests that it could be used to target cancer cells alone, with minor effects on normal surrounding tissues. In addition, we observed the same *in vitro* sensitivity to fusicoccin A on two glioma cell lines despite their different levels of resistance to pro-apoptotic stimuli. The fact that fusicoccin A overcomes, at least partly, the intrinsic resistance of GBM cells to pro-apoptotic stimuli relates to the cytostatic, not cytotoxic, properties of this compound. Indeed, we demonstrated that the fusicoccin A–induced growth inhibitory effects in malignant glioma cells are related to an increase in the duration of cell division.

Fusicoccin A–induced cytostatic effects occur through modifications of actin cytoskeletal organization, a feature that, in turn, can be explained in part by the fact that fusicoccin A inhibits the activity of several kinases necessary for controlling actin cytoskeletal organization. Indeed, inhibiting various protein kinases, such as FAK and ephrins (four of them are targeted by fusicoccin A; Figure 6*A*), perturbs Rho GTPase signaling and therefore alters actin cytoskeletal organization through the Rho/ROCK-dependent formation of actin stress fibers [46,47]. Lamalice et al. demonstrated that the activation of the tyrosine kinase receptor, vascular endothelial growth factor receptor 2 (also targeted by fusicoccin A; Figure 6*A*), by vascular endothelial growth factor leads to actin polymerization and reorganization into stress fibers in endothelial cells [48]. Another kinase inhibited by fusicoccin A is C-Src kinase (CSK), which plays a critical role in mediating G-protein signaling in actin cytoskeletal reorganization [49]. Therefore, the majority of the dozen of kinases impaired by fusicoccin A (Figure 6*A*) are tyrosine

A

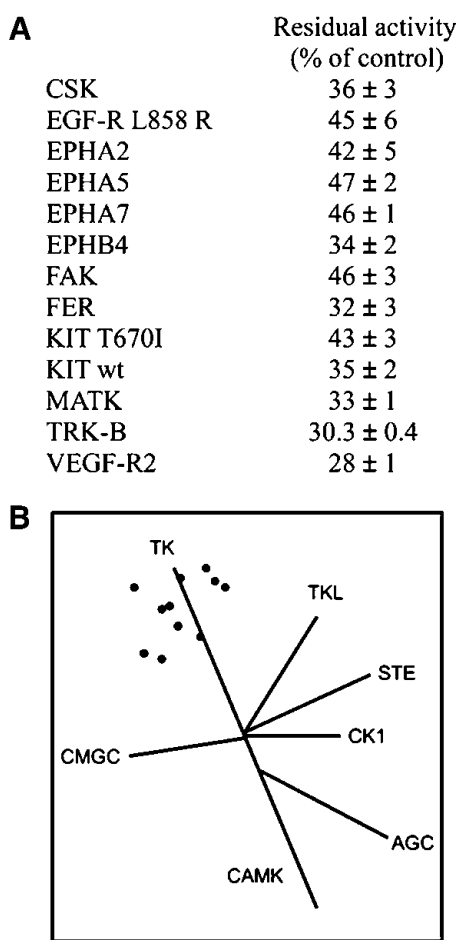|	Residual activity (% of control)
CSK	36 ± 3
EGF-R L858 R	45 ± 6
EPHA2	42 ± 5
EPHA5	47 ± 2
EPHA7	46 ± 1
EPHB4	34 ± 2
FAK	46 ± 3
FER	32 ± 3
KIT T670I	43 ± 3
KIT wt	35 ± 2
MATK	33 ± 1
TRK-B	30.3 ± 0.4
VEGF-R2	28 ± 1

Figure 6. Characterization of fusicoccin A–induced anti-kinase activity. (A) *In vitro* anti-kinase profiles of fusicoccin A. The data are presented as the means ± SD values calculated in duplicate. (B) A schematic illustration of the kinases in the human dendrogram-related kinome that were targeted at 50 μM fusicoccin A with analyses of <50% of kinase residual activity. The various classes of kinases included tyrosine kinases (TK), tyrosine kinase–like kinases (TKL), serine/threonine protein kinases (STE), casein kinases (CK1), cyclic adenosine monophosphate (cAMP)–dependent protein kinases (AGC), calcium/calmodulin protein kinase II kinases (CAMK), and the CMGC subclass, which includes cyclin-dependent kinase, MAPK, glycogen synthase kinase, and cyclin-dependent kinase–like groups of kinases.
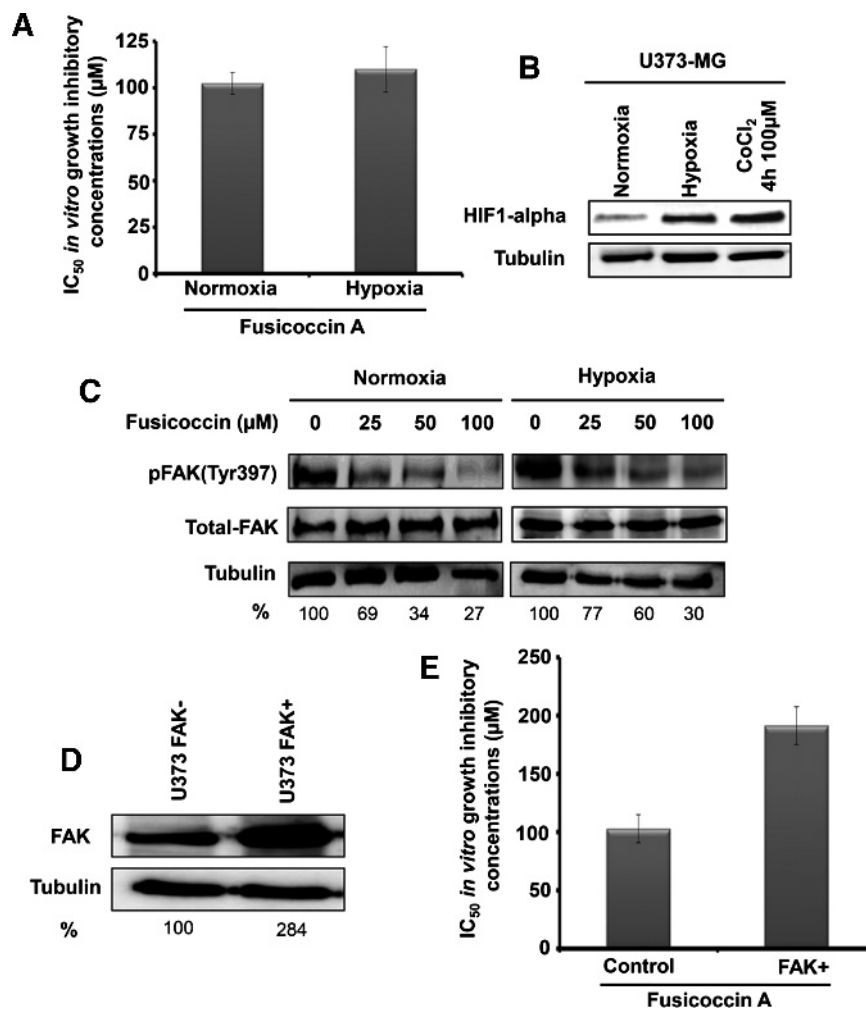
Figure 7. Characterization of fusicoccin A–induced anti-kinase activity, with a focus on FAK. (A) Determination of the *in vitro* IC_{50} of fusicoccin A in U373-MG cells cultured under normoxic and hypoxic conditions using the MTT colorimetric assay. The data are reported as the mean values $\pm$ SD calculated in triplicate. (B) U373-MG cells were incubated under normoxic *versus* hypoxic conditions for 24 hours. $CoCl_2$-treated U373-MG cells were used as a positive control for HIF-1α expression. Total cell lysates were resolved on SDS-PAGE and immunoblotted with the anti–HIF-1α antibody. (C) U373-MG cells either untreated or treated with 25, 50, or 100 μM fusicoccin A for 24 hours were incubated under normoxic or hypoxic culture conditions. Total cell lysates were resolved on SDS-PAGE and immunoblotted with anti–pFAK, total anti-FAK, and anti-tubulin antibodies. The Western blot bands have been digitized, and quantitative data below the Western blot bands represent the number of pixels of the pFAK band multiplied by pixel intensity, the final result of which has been normalized to the corresponding tubulin band. (D) Immunoblot analysis demonstrated FAK overexpression in U373-MG cells when transfected with pCMV6-PTK2 (FAK); pCMV6-XL4 was used for control. The Western blot bands have been digitized, and quantitative data below the Western blot bands represent the number of pixels of the FAK band multiplied by pixel intensity, the final result of which has been normalized to the corresponding tubulin band. (E) Characterization of the *in vitro* growth inhibitory effects induced by fusicoccin A in U373-MG cells transfected with pCMV6-XL4 (control) and pCMV6-PTK2 (FAK).

kinases (Figure 6*B*), which are involved in the migratory and invasive features of malignant glioma cells [44,46,50–53].

Of the various kinases that are impaired by fusicoccin A, we focused on FAK, which is a nonreceptor cytoplasmic tyrosine kinase that is recruited at an early stage to focal adhesions [39]. Various stimuli can induce activation of FAK by autophosphorylation on a particular tyrosine residue, Y397, including integrin and growth factor receptor engagement [39]. Activated FAK creates a high-affinity binding site for Src homology 2 domain–containing proteins that subsequently interact with a number of downstream signaling proteins such as the adaptor protein Grb2 and PI3K [37,39]. Consequently, FAK plays a critical role in malignant GBM cell behavior because it is involved in the regulation of GBM cell growth and survival through the acti-

vation of the PI3K/AKT/mammalian target of rapamycin (mTOR) and the extracellular signal–regulated kinase/MAPK signaling pathways [2,37]. Furthermore, several studies report that FAK is overexpressed in cancer cells, including GBM cells, and that the status of FAK correlates with tumor progression and poor clinical outcomes [44,54]. On the basis of the central function of FAK and its ability to regulate different pathways implicated in dismal prognosis of GBM, FAK represents a target of interest, which is further reinforced by the failure of receptor tyrosine kinase inhibitors.

In GBMs, necrotic foci are surrounded by "pseudopalisading" cells, which are severely hypoxic [55]. Hypoxia in GBM is correlated with aggressiveness and invasiveness by the switch in metabolism, resistance to apoptosis, and neovascularization. All of these phenomena induce

the apparition of TMZ resistance in hypoxic areas [56]. Furthermore, GBM cells are maintained by cancer stem cells that are inherently radiotherapy and chemotherapy resistant and may be preserved *in vivo* in a niche characterized by hypoxia [57,58]. Thus, testing fusicoccin A in different *in vitro* and *in vivo* models containing cancer stem cells, to prove the activity of our molecule on this subtype of cells, would be interesting. Moreover, Skuli et al. [43] have also shown that the integrin/FAK pathway is involved in hypoxic regulation in GBMs. In our report, we found that the hypoxic state of GBM cells does not impair *in vitro* fusicoccin A–induced growth inhibitory activity or its inhibitory effects on FAK activity.

Finally, it should be emphasized that the coefficient partition of fusicoccin A in hydrophilic/lipophilic solutions is more favorable than that of most natural antitumor compounds. Indeed, the theoretical predicted log P value (software calculation) of fusicoccin A is 3.4, which suggests that this compound should be able to cross the blood-brain barrier without the need to tremendously adapt its formulation.

In conclusion, this report identifies fusicoccin A, a fungal metabolite, as an *in vitro* cytostatic and antimigratory compound in human GBM cells that display varying degrees of resistance to pro-apoptotic stimuli. Importantly, fusicoccin A maintains its therapeutic activity in targeting FAK, at least partly, even under hypoxic conditions and displays bioselectivity between normal and tumor glial cells. Altogether, these data open new perspectives for GBM treatment and in particular warrant further studies examining the *in vivo* effects of fusicoccin A on TMZ-resistant brain tumors.

References
[1] Louis DN, Ohgaki H, Wiestler OD, Cavenee WK, Burger PC, Jouvet A, Scheithauer BW, and Kleihues P (2007). The 2007 WHO classification of tumours of the central nervous system. *Acta Neuropathol* **114**, 97–109.
[2] Furnari FB, Fenton T, Bachoo RM, Mukasa A, Stommel JM, Stegh A, Hahn WC, Ligon KL, Louis DN, Brennan C, et al. (2007). Malignant astrocytic glioma: genetics, biology, and paths to treatment. *Genes Dev* **21**, 2683–2710.
[3] Stupp R, Hegi ME, Mason WP, van den Bent MJ, Taphoorn MJ, Janzer RC, Ludwin SK, Allgeier A, Fisher B, Belanger K, et al. (2009). Effects of radiotherapy with concomitant and adjuvant temozolomide versus radiotherapy alone on survival in glioblastoma in a randomised phase III study: 5-year analysis of the EORTC-NCIC trial. *Lancet Oncol* **10**, 459–466.
[4] Louis DN (2006). Molecular pathology of malignant gliomas. *Annu Rev Pathol* **1**, 97–117.
[5] Parsons DW, Jones S, Zhang X, Lin JC, Leary RJ, Angenendt P, Mankoo P, Carter H, Siu IM, Gallia GL, et al. (2008). An integrated genomic analysis of human glioblastoma multiforme. *Science* **321**, 1807–1812.
[6] Yung WK, Vredenburgh JJ, Cloughesy TF, Nghiemphu P, Klencke B, Gilbert MR, Reardon DA, and Prados MD (2010). Safety and efficacy of erlotinib in first-relapse glioblastoma: a phase II open-label study. *Neuro Oncol* **12**, 1061–1070.
[7] De Fazio S, Russo E, Ammendola M, Donato Di Paola E, and De Sarro G (2012). Efficacy and safety of bevacizumab in glioblastomas. *Curr Med Chem* **19**, 972–981.
[8] Gilbert MR, Kuhn J, Lamborn KR, Lieberman F, Wen PY, Mehta M, Cloughesy T, Lassman AB, Deangelis LM, Chang S, et al. (2012). Cilengitide in patients with recurrent glioblastoma: the results of NABTC 03-02, a phase II trial with measures of treatment delivery. *J Neurooncol* **106**, 147–153.
[9] Greve H, Mohamed IE, Pontius A, Kehraus S, Gross H, and Konig GM (2010). Fungal metabolites: structural diversity as incentive for anticancer drug development. *Phytochem Rev* **9**, 537–545.
[10] Newman DJ and Cragg GM (2012). Natural products as sources of new drugs over the 30 years from 1981 to 2010. *J Nat Prod* **75**, 311–335.
[11] Fountzilas G, Karavelis A, Capizzello A, Kalogera-Fountzila A, Karkavelas G, Zamboglou N, Selviaridis P, Foroglou G, and Tourkantonis A (1999). Radiation and concomitant weekly administration of paclitaxel in patients with glioblastoma multiforme. A phase II study. *J Neurooncol* **45**, 159–165.
[12] Vredenburgh JJ, Desjardins A, Reardon DA, and Friedman HS (2009). Experience with irinotecan for the treatment of malignant glioma. *Neuro Oncol* **11**, 80–91.
[13] Fruehauf JP, Brem H, Brem S, Sloan A, Barger G, Huang W, and Parker R (2006). *In vitro* drug response and molecular markers associated with drug resistance in malignant gliomas. *Clin Cancer Res* **12**, 4523–4532.
[14] Ballio A, Chain EB, De Leo P, Erlanger BF, Mauri M, and Tonolo A (1964). Fusicoccin: a new wilting toxin produced by *Fusicoccum amygdali*. *Nature* **203**, 297.
[15] Mackintosh C (2004). Dynamic interactions between 14-3-3 proteins and phosphoproteins regulate diverse cellular processes. *Biochem J* **381**, 329–342.
[16] Bunney TD, De Boer AH, and Levin M (2003). Fusicoccin signaling reveals 14-3-3 protein function as a novel step in left-right patterning during amphibian embryogenesis. *Development* **130**, 4847–4858.
[17] Takahashi M, Kawamura A, Jato N, Nishi T, Hamachi I, and Ohkanda J (2012). Phosphopeptide-dependent labeling of 14-3-3ζ proteins by fusicoccin-based fluorescent probes. *Angew Chem Int Ed Engl* **51**, 509–512.
[18] Yang X, Cao W, Lin H, Zhang W, Lin W, Cao L, Zhen H, Huo J, and Zhang X (2009). Isoform-specific expression of 14-3-3 proteins in human astrocytoma. *J Neurol Sci* **276**, 54–59.
[19] de Vries-van Leeuwen IJ, Kortekaas-Thijssen C, Nzigou Mandouckou JA, Kas S, Evidente A, and de Boer AH (2010). Fusicoccin-A selectively induces apoptosis in tumor cells after interferon-α priming. *Cancer Lett* **293**, 198–206.
[20] Ballio A, Carilli A, Santurbano B, and Tuttobello L (1968). Produzione di fusicoccina in scala pilota. *Ann Ist Super Sanita* **4**, 317–332.
[21] Evidente A, Andolfi A, Fiore A, Boari A, and Vurro M (2006). Stimulation of *Orobanche ramosa* seed germination by fusicoccin derivatives: a structure-activity relationship study. *Phytochemistry* **67**, 19–26.
[22] Martinive P, De Wever J, Bouzin C, Baudelet C, Sonveaux P, Grégoire V, Gallez B, and Feron O (2006). Reversal of temporal and spatial heterogeneities in tumor perfusion identifies the tumor vascular tone as a tunable variable to improve drug delivery. *Mol Cancer Ther* **5**, 1620–1627.
[23] Lee S, Qiao J, Paul P, O'Connor KL, Evers BM, and Chung DH (2012). FAK is a critical regulator of neuroblastoma liver metastasis. *Oncotarget*.
[24] Mosmann T (1983). Rapid colorimetric assay for cellular growth and survival: application to proliferation and cytotoxicity assays. *J Immunol Methods* **65**, 55–63.
[25] Debeir O, Mégalizzi V, Warzée N, Kiss R, and Decaestecker C (2008). Video-microscopic extraction of specific information on cell proliferation and migration in vitro. *Exp Cell Res* **314**, 2985–2998.
[26] Mégalizzi V, Decaestecker C, Debeir O, Spiegl-Kreinecker S, Berger W, Lefranc F, Kast RE, and Kiss R (2009). Screening of anti-glioma effects induced by sigma-1 receptor ligands: potential new use for old anti-psychiatric medicines. *Eur J Cancer* **45**, 2893–2905.
[27] Debeir O, Van Ham P, Kiss R, and Decaestecker C (2005). Tracking of migrating cells under phase-contrast video microscopy with combined mean-shift processes. *IEEE Trans Med Imaging* **24**, 697–711.
[28] Le Calvé B, Lallemand B, Perrone C, Lenglet G, Depauw S, Van Goietsenoven G, Bury M, Vurro M, Herphelin F, Andolfi A, et al. (2011). In vitro anticancer activity, toxicity and structure-activity relationships of phyllostictine A, a natural oxazatricycloalkenone produced by the fungus *Phyllosticta cirsii*. *Toxicol Appl Pharmacol* **254**, 8–17.
[29] Lallemand B, Chaix F, Bury M, Bruyère C, Ghostin J, Becker JP, Delporte C, Gelbcke M, Mathieu V, Dubois J, et al. (2011). *N*-(2-{3-[3,5-bis(trifluoromethyl)phenyl]ureido}ethyl)-glycyrrhetinamide (6b): a novel anticancer glycyrrhetinic acid derivative that targets the proteasome and displays anti-kinase activity. *J Med Chem* **54**, 6501–6513.
[30] Mégalizzi V, Mathieu V, Mijatovic T, Gailly P, Debeir O, De Neve N, Van Damme M, Bontempi G, Haibe-Kains B, Decaestecker C, et al. (2007). 4-IBP, a sigma1 receptor agonist, decreases the migration of human cancer cells, including glioblastoma cells, *in vitro* and sensitizes them *in vitro* and *in vivo* to cytotoxic insults of proapoptotic and proautophagic drugs. *Neoplasia* **9**, 358–369.
[31] Le Mercier M, Fortin S, Mathieu V, Roland I, Spiegl-Kreinecker S, Haibe-Kains B, Bontempi G, Decaestecker C, Berger W, Lefranc F, et al. (2009). Galectin 1 proangiogenic and promigratory effects in the Hs683 oligodendroglioma model are partly mediated through the control of BEX2 expression. *Neoplasia* **11**, 485–496.

[32] Lamoral-Theys D, Wauthoz N, Heffeter P, Mathieu V, Jungwirth U, Lefranc F, Nève J, Dubois J, Dufrasne F, Amighi K, et al. (2012). Trivanillic polyphenols with anticancer cytostatic effects through the targeting of multiple kinases and intracellular Ca^{2+} release. *J Cell Mol Med* **16**, 1421–1434.

[33] Gomez-Manzano C, Fueyo J, Kyritsis AP, McDonnell TJ, Steck PA, Levin VA, and Yung WK (1997). Characterization of p53 and p21 functional interactions in glioma cells en route to apoptosis. *J Natl Cancer Inst* **89**, 1036–1044.

[34] Dittmann LM, Danner A, Gronych J, Wolter M, Stühler K, Grzendowski M, Becker N, Bageritz J, Goidts V, Toedt G, et al. (2012). Downregulation of PRDX1 by promoter hypermethylation is frequent in 1p/19q-deleted oligo-dendroglial tumours and increases radio- and chemosensitivity of Hs683 glioma cells *in vitro*. *Oncogene* **31**, 3409–3418.

[35] Carragher NO and Frame MC (2004). Focal adhesion and actin dynamics: a place where kinases and proteases meet to promote invasion. *Trends Cell Biol* **14**, 241–249.

[36] Traxler P (2003). Tyrosine kinases as targets in cancer therapy—successes and failures. *Expert Opin Ther Targets* **7**, 215–234.

[37] McLean GW, Carragher NO, Avizienyte E, Evans J, Brunton VG, and Frame MC (2005). The role of focal-adhesion kinase in cancer—a new therapeutic opportunity. *Nat Rev Cancer* **5**, 505–515.

[38] Zhao X and Guan JL (2003). Focal adhesion kinase and its signaling pathways in cell migration and angiogenesis. *Adv Drug Deliv Rev* **63**, 610–615.

[39] Parsons JT (2003). Focal adhesion kinase: the first ten years. *J Cell Sci* **116**, 1409–1416.

[40] Kim LC, Song L, and Haura EB (2009). Src kinases as therapeutic targets for cancer. *Nat Rev Clin Oncol* **6**, 587–595.

[41] Xu LH, Owens LV, Sturge GC, Yang X, Liu ET, Craven RJ, and Cance WG (1996). Attenuation of the expression of the focal adhesion kinase induces apoptosis in tumor cells. *Cell Growth Differ* **7**, 413–418.

[42] Gabarra-Niecko V, Schaller MD, and Dunty JM (2003). FAK regulates biological processes important for the pathogenesis of cancer. *Cancer Metastasis Rev* **22**, 359–374.

[43] Skuli N, Monferran S, Delmas C, Favre G, Bonnet J, Toulas C, and Cohen-Jonathan Moyal E (2009). $\alpha_v\beta_3/\alpha_v\beta_5$ Integrins-FAK-RhoB: a novel pathway for hypoxia regulation in glioblastoma. *Cancer Res* **69**, 3308–3316.

[44] Natarajan M, Hecker TP, and Gladson CL (2003). FAK signaling in anaplastic astrocytoma and glioblastoma tumors. *Cancer J* **9**, 126–133.

[45] Reardon DA, Rich JN, Friedman HS, and Bigner DD (2006). Recent advances in the treatment of malignant astrocytoma. *J Clin Oncol* **24**, 1253–1265.

[46] Nakada M, Hayashi Y, and Hamada J (2011). Role of Eph/ephrin tyrosine kinase in malignant glioma. *Neuro Oncol* **13**, 1163–1170.

[47] Torsoni AS, Marin TM, Velloso LA, and Franchini KG (2005). RhoA/ROCK signaling is critical to FAK activation by cyclic stretch in cardiac myocytes. *Am J Physiol Heart Circ Physiol* **289**, 1488–1496.

[48] Lamalice L, Houle F, Jourdan G, and Huot J (2004). Phosphorylation of tyrosine 1214 on VEGFR2 is required for VEGF-induced activation of Cdc42 upstream of SAPK2/p38. *Oncogene* **23**, 434–445.

[49] Lowry WE, Huang J, Ma YC, Ali S, Wang D, Williams DM, Okada M, Cole PA, and Huang XY (2002). Csk, a critical link of g protein signals to actin cytoskeletal reorganization. *Dev Cell* **2**, 733–744.

[50] Angers-Loustau A, Hering R, Werbowetski TE, Kaplan DR, and Del Maestro RF (2004). SRC regulates actin dynamics and invasion of malignant glial cells in three dimensions. *Mol Cancer Res* **2**, 595–605.

[51] Wadhwa S, Nag TC, Jindal A, Kushwaha R, Mahapatra AK, and Sarkar C (2003). Expression of the neurotrophin receptors Trk A and Trk B in adult human astrocytoma and glioblastoma. *J Biosci* **28**, 181–188.

[52] Sjöström S, Wibom C, Andersson U, Brännström T, Broholm H, Johansen C, Collatz-Laier H, Liu Y, Bondy M, Henriksson R, et al. (2011). Genetic variations in VEGF and VEGFR2 and glioblastoma outcome. *J Neurooncol* **104**, 523–527.

[53] Lipinski CA, Tran NL, Menashi E, Rohl C, Kloss J, Bay RC, Berens ME, and Loftus JC (2005). The tyrosine kinase pyk2 promotes migration and invasion of glioma cells. *Neoplasia* **7**, 435–445.

[54] Siesser PM and Hanks SK (2006). The signaling and biological implications of FAK overexpression in cancer. *Clin Cancer Res* **12**, 3233–3237.

[55] Rong Y, Durden DL, Van Meir EG, and Brat DJ (2006). 'Pseudopalisading' necrosis in glioblastoma: a familiar morphologic feature that links vascular pathology, hypoxia, and angiogenesis. *J Neuropathol Exp Neurol* **65**, 529–539.

[56] Pistollato F, Abbadi S, Rampazzo E, Persano L, Della Puppa A, Frasson C, Sarto E, Scienza R, D'avella D, and Basso G (2010). Intratumoral hypoxic gradient drives stem cells distribution and MGMT expression in glioblastoma. *Stem Cells* **28**, 851–862.

[57] Bar EE (2011). Glioblastoma, cancer stem cells and hypoxia. *Brain Pathol* **21**, 119–129.

[58] Frosina G (2011). Frontiers in targeting glioma stem cells. *Eur J Cancer* **47**, 496–507.